25th ABCM International Congress of Mechanical Engineering
October 20-25, 2019, Uberlândia, MG, Brazil

DYNAMIC MODELLING AND CONTROL OF UNMANNED AERIAL VEHICLE OF THE QUADROTOR TYPE

Allan Carlos Ferreira de Oliveira
José Alberto Torrico Altuna
Federal University of ABC Engineering, Modeling and Applied Social Sciences Center (CECS), Santo André, Brazil.
allancfo2012@gmail.com; jose.torrico@ufabc.edu.br

Diego Paolo Ferruzzo Correa
Federal University of ABC Engineering, Modeling and Applied Social Sciences Center (CECS), São Bernardo dos Campos, Brazil.
diego.ferruzzo@ufabc.edu.br

Abstract.*This paper presents a dynamic model for an Unmanned Aerial Vehicle of the quadrotor type, together with the design of proportional controllers and based on the State-Dependent Riccati Equation (SDRE) to control the vehicle's velocities and to stabilize the attitude, respectively. The mathematical model is obtained by the Newtonian formalism considering the gyroscopic effect as disturbance input to the system, the translational and rotational dynamics are described in the inertial frame. Different from most of the works in literature which only consider small-angles variation simplifications, in this contribution the analysis is done considering the full nonlinear dynamic, which results in the coupling of control inputs to the rotational system. The designed controllers are applied in two flight situations: rectilinear and spiral trajectories, both with manually adjusted gains. The results show that relative error in the x-y-z final position are approximately 0.1%, 0.07% and 0.22%, for the first trajectory, and 0.24%, 7% and 1.08% for the second trajectory, being for y the exact error. In addition, the influence of the gyroscopic effect with position error of the order* 10^{-5}*m was verified.*

Keywords: *Unmanned Aerial Vehicle (UAV), quadrotor, State-Dependent Riccati Equation (SDRE), gyroscopic effect*

1. INTRODUCTION

The interest in Unmanned Aerial Vehicles (UAVs) has intensified in recent years, due to their versatility and low cost, which made them suitable for applications as the reduction of human exposure to long, monotonous and dangerous tasks, as well as provide possible financial savings and environmental benefits (e.g. reduction of fuel consumption and less CO_2 emissions) (MDIC (2017)). Its main applications in the civil and industrial fields are: firefighting; border monitoring; detection of soil erosion and infrastructure defects; crop spraying; deliveries and in the film industry. Considering their type, UAV platforms typically fall into one of the following four categories: fixed-wing; rotary-wing; blimps and flapping-wings (Nonami *et al.* (2010)). The aircrafts classified in the second group, such as quadrotor and helicopter, have a set of characteristics that make them more attractive when compared with other vehicles: they can hover at a certain altitude, have a high degree of manoeuvrability and perform vertical take-off and landing,which allows indoor exploration and irregular surfaces.

However, the mentioned advantages are offset by the difficulty in designing the control systems. This is due to the fact that this vehicle is a sub-actuated mechanical system, i.e., it has six degrees of freedom, three position coordinates (x, y, and z) and three orientation angles (ϕ, θ and ψ), and only four control inputs (speed of the four rotors). In addition, they are highly nonlinear, affected by aerodynamic disturbances, and are subject to parametric uncertainties as well as unmodeled dynamics (Lima *et al.* (2014)).

A quadrotor consists of four rotors, each fitted at one end of a cross-like structure. Each rotor consists of a propeller fitted to a separately powered DC motor. Propellers 1 and 3 rotate in the same direction while propellers 2 and 4 rotate in an opposite direction to reduce the gyroscopic effect (ElKholy (2014)). By increasing or decreasing the speed of the four propellers simultaneously, it is possible to vary its altitude. By maintaining the speeds of the propellers 1 and 3, and by changing the speed of 2 and 4, a rotation about the x axis (roll moment) is generated, producing a movement along its y axis. Considering the speeds of the propellers 2 and 4 constant and modifying the speed of 1 and 3, a rotation is obtained around the y axis (pitch moment) and consequently the vehicle moves along its axis x. Finally, to perform a rotation about the z axis (yaw moment), it is necessary to increase the speed of one of the pairs of propellers together with the reduction of the speed of the other pair.

This paper presents the nonlinear dynamic model for a quadrotor using the Newtonian formalism without considering the simplification of small angular variations commonly found in the literature. The hypotheses assumed in the modelling

process are: the quadrotor is a rigid body and it has a symmetrical structure; the four motors are identical, as also are the four propellers; the ground effect is neglected; the gyroscopic effect is considered and the thrust force and the drag moment are proportional to the square of the propeller's angular speed. As control strategy, the proposal presented in paper Voos (2006) is adopted, where an outer-loop controller is associated to the translation velocities, for this aim proportional controllers are used, and an inner control loop is related to attitude control, for this purpose the SDRE (State Dependent Riccati Equation) controller is applied. This strategy becomes interesting for certain applications, in which the operator, through a human-machine interface, obtains flexibility in the navigation of the platform and the robustness in the tracking of the attitude. The simulations will show that although the nonlinear terms result in the behaviour more oscillatory of Euler angulars , the adopted control strategy allowed to achieve satisfactory results for the desired flight paths. In addition, a small influence of the gyroscopic effect in position error was verified. This result is justified by the fact that the motor has a small moment of inertia, and therefore, it is possible to neglect it in these cases.

This paper is organized as follows. *Dynamic model of the quadrotor* section includes definitions that are used in mathematical modelling and the equations that describe the dynamics of the quadrotor. *Control System* section highlights the main points of the SDRE theory and the control methodology adopted. The simulations for two flight paths and the influence of the gyroscopic effect are shown in *Numerical Results* section. Finally, the conclusions are presented.

2. DYNAMIC MODEL OF THE QUADROTOR

In order to elaborate the dynamic model, it is necessary to define two coordinate systems: the inertial referential system (E), located at ground level, and the body system (B), whose origin coincides with the center of mass of the structure. A representation of both is shown in Fig. 1.

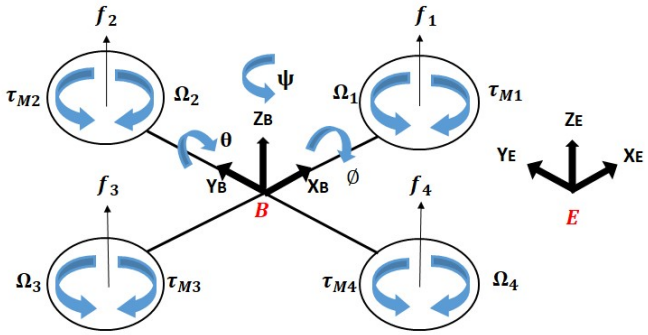

Figure 1. Inertial referential (E) and body (B) coordinate systems.

The relationship between these systems occurs through three successive rotations along the axes, being represented by Euler angles, where ϕ is the roll angle, θ is the pitch angle, and ψ is the yaw angle. The rotation sequence can be considered in any order, however the most commonly used in aeronautics is the sequence 3-2-1, also known as Z-Y-X (Da Silva (2012)). The first rotation occurs around the Z_E axis, expressed by an angle ψ, resulting in an intermediate system OX'Y'Z'. Subsequently, an angular displacement θ is carried out around the Y', generating the second intermediate system OX"Y"Z" . Finally, by rotating the X" axis by an angle ϕ, the parallelism between the two coordinate systems is reached. Mathematically, these rotations are indicated as follows

$$\mathbf{R}(\psi) = \begin{bmatrix} \cos(\psi) & \sin(\psi) & 0 \\ -\sin(\psi) & \cos(\psi) & 0 \\ 0 & 0 & 1 \end{bmatrix}, \quad \mathbf{R}(\theta) = \begin{bmatrix} \cos(\theta) & 0 & -\sin(\theta) \\ 0 & 1 & 0 \\ \sin(\theta) & 0 & \cos(\theta) \end{bmatrix}, \quad \mathbf{R}(\phi) = \begin{bmatrix} 1 & 0 & 0 \\ 0 & \cos(\phi) & \sin(\phi) \\ 0 & -\sin(\phi) & \cos(\phi) \end{bmatrix}.$$

The product of the three matrices, $\boldsymbol{R}(\phi)\ \boldsymbol{R}(\theta)\ \boldsymbol{R}(\psi)$, results in a matrix $\boldsymbol{R}_E^B$ that describes the vector projection of the inertial reference system to the system connected to the rigid body. The matrix of $\boldsymbol{R}_E^B$ is orthogonal, this means that $(\boldsymbol{R}_E^B)^{-1} = (\boldsymbol{R}_E^B)^T$, where the matrix $(\boldsymbol{R}_E^B)^{-1}$ corresponds to the rotation matrix of the vectors from the coordinate system of the body to the inertial coordinate one, represented by equation (1) where S_k = sin(k) and C_k = cos (k).

$$(\boldsymbol{R}_E^B)^{-1} = \begin{bmatrix} C_\theta C_\psi & S_\phi S_\theta C_\psi - C_\phi S_\psi & C_\phi S_\theta C_\psi + S_\phi S_\psi \\ C_\theta S_\psi & S_\phi S_\theta S_\psi + C_\phi C_\psi & C_\phi S_\theta S_\psi - S_\phi C_\psi \\ -S_\theta & C_\theta S_\phi & C_\theta C_\phi \end{bmatrix} \tag{1}$$

The angular velocity $\boldsymbol{\omega}$ of the quadrotor can be described in both systems, in the body referential and in the inertial one, as shown in equations (2) and (3), respectively. Based on the rotation matrices, we can relate the components of

the angular velocity of the rigid body (p, q, r) to the rates of variation of the Euler angles ($\dot{\phi}$, $\dot{\theta}$, $\dot{\psi}$) from the versor transformation in the inertial and intermediate systems to one of the body system,

$$\boldsymbol{\omega} = p\hat{\boldsymbol{i}}_B + q\hat{\boldsymbol{j}}_B + r\hat{\boldsymbol{k}}_B \tag{2}$$

$$\boldsymbol{\omega} = \dot{\psi}\hat{\boldsymbol{k}}_E + \dot{\theta}\hat{\boldsymbol{j}}' + \dot{\phi}\hat{\boldsymbol{i}}'' \tag{3}$$

where ($\hat{\boldsymbol{i}}_B$,$\hat{\boldsymbol{j}}_B$,$\hat{\boldsymbol{k}}_B$) are versors of the body coordinate system; ($\hat{\boldsymbol{k}}_E$,$\hat{\boldsymbol{j}}'$,$\hat{\boldsymbol{i}}''$) are versors corresponding to the Z_E, Y' and X'' axis, respectively. From this transformation, we arrive at the following relation (Mo and Farid (2019)):

$$\begin{bmatrix}\dot{\phi}\\ \dot{\theta}\\ \dot{\psi}\end{bmatrix} = \boldsymbol{W}\begin{bmatrix}p\\ q\\ r\end{bmatrix} = \begin{bmatrix}1 & T_\theta S_\phi & T_\theta C_\phi\\ 0 & C_\phi & -S_\phi\\ 0 & S_\phi/C_\theta & C_\phi/C_\theta\end{bmatrix}\begin{bmatrix}p\\ q\\ r\end{bmatrix}, \tag{4}$$

where T_k = tan(k).

2.1 Translational and rotational dynamics

The main aerodynamic force responsible for the translational motion is the thrust originated from the rotation of the propellers. Such force acts on the coordinate system of the body, perpendicular to the plane XY along the axis Z. The contribution of each propeller results in the total thrust (T_b) represented by:

$$T_b = \sum_{i=1}^{4} T_i = k_f \sum_{i=1}^{4} {\Omega_i}^2,$$

where Ω_i is the angular velocity of the respective propeller and k_f is a proportionality constant. Applying the Newton's second law, the translational dynamic described in inertial frame is given by:

$$m_t\dot{\boldsymbol{v}} = \boldsymbol{P} + (\boldsymbol{R}_{\boldsymbol{E}}^{\boldsymbol{B}})^{-1}\begin{bmatrix}0 & 0 & T_b\end{bmatrix}^T \tag{5}$$

where $P = [0 \quad 0 \quad mg]^T$ is the gravitational force, m_t is the mass of the vehicle, g is gravitational acceleration: $g = 9.81m/s^2$ and $\dot{\boldsymbol{v}}$ is the linear acceleration.

Three types of moments are considered acting on the quadrotor: one resulting of the application of thrust; drag one of each propeller and gyroscopic one. Considering motors 1 and 3, located along the X axis, the moment resulting from the respective forces is given by:

$$M_{pitch} = T_3L - T_1L = k_fL({\Omega_3}^2 - {\Omega_1}^2),$$

where L is distance between the center of mass and the axis of rotation of the motor. The same reasoning can be applied to calculate the moments generated by the motors 2 and 4 along the Y axis, whose resultant one referring to the two forces, is expressed by:

$$M_{roll} = T_2L - T_4L = k_fL({\Omega_2}^2 - {\Omega_4}^2).$$

The moment yaw is defined by the sum of the drag moment of each propeller (τ_{Mi}). The direction of rotation of the propeller defines the signal of the drag moment, a positive one is generated by a clockwise propeller rotation, a negative one is generate when the rotation is counter clockwise:

$$M_{yaw} = \sum_{i=1}^{4} \tau_{Mi}(-1)^i = k_m \sum_{i=1}^{4} {\Omega_i}^2(-1)^i,$$

where k_m is an aerodynamic constant. The gyroscopic moment is a physical effect that is associated with rotors' inertia. The axes of these motors (spin axes) are parallel to Z axis of the platform. When the quadrotor performs a roll or pitch movement it changes the direction of the angular momentum vectors of the four motors. The result is a gyroscopic moment that attempts to turn the spin axis so that it aligns with rotation around the Z axis (Derafa *et al.* (2006)). Quantitatively, this moment can be described as

$$\boldsymbol{M_G} = \boldsymbol{\omega} \times \begin{bmatrix}0\\ 0\\ I_r\Omega_r\end{bmatrix} = \begin{bmatrix}qI_r\Omega_r\\ -pI_r\Omega_r\\ 0\end{bmatrix},$$

where I_r is the moment of rotor's inertia and Ω_r propeller's relative speed $\Omega_r = (-\Omega_1 + \Omega_2 - \Omega_3 + \Omega_4)$. Using the Newton's second law, the rotational dynamic is given by:

$$\boldsymbol{I}\dot{\boldsymbol{\omega}} + \boldsymbol{\omega} \times (\boldsymbol{I}\boldsymbol{\omega}) = \boldsymbol{M} = \begin{bmatrix} M_x \\ M_y \\ M_z \end{bmatrix} = \begin{bmatrix} M_{roll} \\ M_{pitch} \\ M_{yaw} \end{bmatrix} - \boldsymbol{M_G}, \tag{6}$$

where $\boldsymbol{M}$ is the total torque and $\boldsymbol{I}$ is the inertia matrix of the structure. Based on the assumption that the quadrotor has symmetric mass distribution, the matrix $\boldsymbol{I}$ becomes diagonal matrix (Chovancová *et al.* (2014)). From the Eq. (6), the angular acceleration in the body system can be written as:

$$\dot{\boldsymbol{\omega}} = \boldsymbol{I}^{-1}(\boldsymbol{M} - \boldsymbol{\omega} \times (\boldsymbol{I}\boldsymbol{\omega})). \tag{7}$$

To represent it in the inertial reference system, one can derive the Eq. (4):

$$\begin{bmatrix} \ddot{\phi} \\ \ddot{\theta} \\ \ddot{\psi} \end{bmatrix} = \frac{\mathrm{d}(\boldsymbol{W}\boldsymbol{\omega})}{\mathrm{d}t} = \frac{\mathrm{d}(\boldsymbol{W})}{\mathrm{d}t}\boldsymbol{\omega} + \boldsymbol{W}\dot{\boldsymbol{\omega}} \tag{8}$$

By replacing the forces and the rotation matrix in Eq. (5) and expanding the Eq. (8), we arrive in the equations that describes dynamic of the quadrotor,

$$\ddot{x} = \frac{1}{m_t}(C_\phi S_\theta C_\psi + S_\phi S_\psi)T_b \tag{9}$$

$$\ddot{y} = \frac{1}{m_t}(C_\phi S_\theta S_\psi - S_\phi C_\psi)T_b \tag{10}$$

$$\ddot{z} = -g + \frac{1}{m_t}(C_\phi C_\theta)T_b \tag{11}$$

$$\ddot{\phi} = a_1\dot{\phi}\dot{\theta} + a_2\dot{\phi}\dot{\psi} + a_3\dot{\theta}\dot{\psi} + a_4\dot{\theta}^2 + a_5\dot{\psi}^2 + b_1M_{roll} + b_2M_{pitch} + b_3M_{yaw} + c_1\dot{\theta} + c_2\dot{\psi} + c_3\dot{\phi} \tag{12}$$

$$\ddot{\theta} = a_6\dot{\phi}\dot{\theta} + a_7x\dot{\phi}\dot{\psi} + a_8\dot{\theta}\dot{\psi} + a_9\dot{\psi}^2 + b_4M_{pitch} + b_5M_{yaw} + c_4\dot{\psi} + c_5\dot{\phi} \tag{13}$$

$$\ddot{\psi} = a_{10}\dot{\phi}\dot{\theta} + a_{11}x\dot{\phi}\dot{\psi} + a_{12}\dot{\theta}\dot{\psi} + a_{13}\dot{\psi}^2 + b_6M_{pitch} + b_7M_{yaw} + c_6\dot{\psi} + c_7\dot{\phi} \tag{14}$$

The coefficients a_i and b_i are related to the Euler angles and moment of inertia of the quadrotor while the coefficients c_i present the same dependence, in addition to the terms associated to gyroscopic effect. These coefficients can be seen in work (De Oliveira (2019)).

The translational and rotational dynamics can be rewritten in the form of state space $\dot{\boldsymbol{X}} = f(\boldsymbol{X}, \boldsymbol{U})$, where $\boldsymbol{U}$ is control input vector, whose inputs are designated by $U_1 = T_b$; $U_2 = M_{roll}$; $U_3 = M_{pitch}$ e $U_4 = M_{yaw}$, and $\boldsymbol{X}$ is the state variables vector chosen as follows:

$$\boldsymbol{X} = \begin{bmatrix} x & \dot{x} & y & \dot{y} & z & \dot{z} & \phi & \dot{\phi} & \theta & \dot{\theta} & \psi & \dot{\psi} \end{bmatrix}^T.$$

From Eq. (9) to (14), we have:

$$\dot{x}_1 = x_2$$
$$\dot{x}_2 = \frac{1}{mt}(cos(x_7)sin(x_9)cos(x_{11}) + sin(x_7)sin(x_{11})U_1$$
$$\dot{x}_3 = x_4$$
$$\dot{x}_4 = \frac{1}{mt}(cos(x_7)sin(x_9)sin(x_{11}) - sin(x_7)cos(x_{11})U_1$$
$$\dot{x}_5 = x_6$$
$$\dot{x}_6 = -g + \frac{1}{mt}(cos(x_7)cos(x_9))U_1$$
$$\dot{x}_7 = x_8$$
$$\dot{x}_8 = a_1x_8x_{10} + a_2x_8x_{12} + a_3x_{10}x_{12} + a_4x_{10}^2 + a_5x_{12}^2 + b_1U_2 + b_2U_3 + b_3U_4 + c_1x_{10} + c_2x_{12} + c_3x_8$$
$$\dot{x}_9 = x_{10}$$
$$\dot{x}_{10} = a_6x_8x_{10} + a_7x_8x_{12} + a_8x_{10}x_{12} + a_9x_{12}^2 + b_4U_3 + b_5U_4 + c_4x_{12} + c_5x_8$$
$$\dot{x}_{11} = x_{12}$$
$$\dot{x}_{12} = a_{10}x_8x_{10} + a_{11}x_8x_{12} + a_{12}x_{10}x_{12} + a_{13}x_{12}^2 + b_6U_3 + b_7U_4 + c_6x_{12} + c_7x_8$$

3. CONTROL SYSTEM

The control strategy is based on the cascade architecture shown in Fig. 2, where the SDRE controller is designed to stabilize the attitude of the vehicle and the proportional controllers are applied to control the velocities in the x, y, and z directions. In Figure 2, blocks C1 and C2 represent the SDRE and the proportional controllers, while blocks M1 and M2 represent the rotational and translational dynamics.

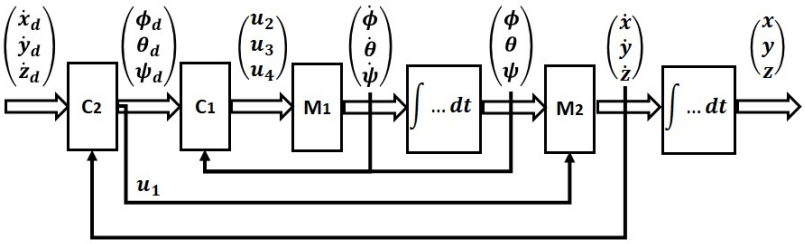

Figure 2. Division of the control system in SDRE and proportional controllers (Voos (2006)).

The idea of the strategy proposed is to relate to the variables that are correlated with the desired velocities x, y and z in direction, i.e., desired roll and pitch angles (x_{7d} and x_{9d}) and total thrust (U_1), and the proportional controllers $\tilde{u}_1 = k_1(\dot{x}_d - \dot{x})$, $\tilde{u}_2 = k_2(\dot{y}_d - \dot{y})$, $\tilde{u}_3 = k_3(\dot{z}_d - \dot{z})$. For this, each controllers will be associated associated to an equation:

$$\frac{1}{mt}(cos(x_7)sin(x_9)cos(x_{11}) + sin(x_7)sin(x_{11})U_1 = \tilde{u}_1,$$

$$\frac{1}{mt}(cos(x_7)sin(x_9)sin(x_{11}) - sin(x_7)cos(x_{11})U_1 = \tilde{u}_2,$$

$$-g + \frac{1}{mt}(cos(x_7)cos(x_9))U_1 = \tilde{u}_3.$$

It is important to highlight that there are three equations and four unknown variables, which makes it possible to adopt a value for one of these variables, in this case, $\phi_d = 0$. That means that the quadrotor is steered without yaw rotation which is not necessary for achieving a desired velocity vector (Voos (2006)). Thus, we arrive at the following relations:

$$U_1 = \frac{m_t(\tilde{u}_3 + g)}{cos(x_{7d})cos(x_{9d})}, \qquad x_{7d} = arctan(\frac{-\tilde{u}_2 cos(x_9 d)}{\tilde{u}_3 + g}), \qquad x_{9d} = arctan(\frac{\tilde{u}_1}{\tilde{u}_3 + g}).$$

Unlike in Voos (2006), the control strategy is realized without considering small-angles simplification.

3.1 State Dependent Riccati Equation (SDRE)

The SDRE methodology is based on the concept of extended linearization to deal with the optimal control problem for nonlinear systems. Extended linearization, also known as SDC parameterization (Mracek and Cloutier (1998)), is a procedure to represent a nonlinear system into a linear one which contains State-Dependent Coefficient (SDC) matrices (Çimen (2008)). Thus, the equation described in the form of state space

$$\dot{\mathbf{x}} = \mathbf{f}(\mathbf{x}) + \mathbf{B}(\mathbf{x})\mathbf{u}$$

can be represented in the form:

$$\dot{\mathbf{x}} = \mathbf{A}(\mathbf{x})\mathbf{x} + \mathbf{B}(\mathbf{x})\mathbf{u}.$$

Among the 512 possible SDC parametrizations of the matrix $\boldsymbol{A}(\boldsymbol{x})$ for the rotational system (De Oliveira (2019)), we choose the following factorization:

$$\boldsymbol{A}(\boldsymbol{x}) = \begin{bmatrix} 0 & 1 & 0 & 0 & 0 & 0 \\ 0 & A_1 & 0 & A_2 & 0 & A_3 \\ 0 & 0 & 0 & 1 & 0 & 0 \\ 0 & A_4 & 0 & A_5 & 0 & A_6 \\ 0 & 0 & 0 & 0 & 0 & 1 \\ 0 & A_7 & 0 & A_8 & 0 & A_9 \end{bmatrix} \qquad \boldsymbol{B}(\boldsymbol{x}) = \begin{bmatrix} 0 & 0 & 0 & 0 \\ 0 & B_1 & B_2 & B_3 \\ 0 & 0 & 0 & 0 \\ 0 & 0 & B_4 & B_5 \\ 0 & 0 & 0 & 0 \\ 0 & 0 & B_6 & B_7 \end{bmatrix}$$

whose coefficients are:

$$A_1 = a_1x_{10} + a_2x_{12} + c_3 \qquad A_2 = a_4x_{10} + c_1$$
$$A_3 = a_3x_{10} + a_5x_{12} + c_2 \qquad A_4 = a_6x_{10} + a_7x_{12} + c_5$$
$$A_5 = a_8x_{12} \qquad A_6 = a_9x_{12} + c_4$$
$$A_7 = a_{10}x_{10} + a_{11}x_{12} + c_7 \qquad A_8 = a_{12}x_{12}$$
$$A_9 = a_{13}x_{12} + c_6 \qquad B_1 = \frac{1}{I_{xx}}$$
$$B_2 = \frac{T_\theta S_\phi}{I_{yy}} \qquad B_3 = \frac{T_\theta C_\phi}{I_{zz}}$$
$$B_4 = \frac{C_\phi}{I_{yy}} \qquad B_5 = \frac{-S_\phi}{I_{zz}}$$
$$B_6 = \frac{S_\phi}{C_\theta I_{yy}} \qquad B_7 = \frac{C_\phi}{C_\theta I_{zz}}$$

It is important to point out that the different choices of $\boldsymbol{A}(\boldsymbol{x})$ create new possibilities to be tested in improvement the controller performance, since for each option of $\boldsymbol{A}(\boldsymbol{x})$, a distinct solution is obtained for the controller (in this case, 511 suboptimal solutions and 1 optimal one). In addition, it must be verified for each parameterization that the controllability of the system is not violated.

In this paper, SDRE controller is used to control the rotational dynamic in such that it occurs tracking of the desired output vector ($\mathbf{y_d}(t)$), thus a performance index is proposed as follows

$$\mathbf{J}(\mathbf{e}(t), \mathbf{u}(t)) = \frac{1}{2}\int_0^\infty (\mathbf{e}^T(t)\mathbf{Q}(\mathbf{x})\mathbf{e}(t) + \mathbf{u}^T(t)\mathbf{R}(\mathbf{x})\mathbf{u}(t))dt \tag{15}$$

where $\mathbf{e}(t) = \mathbf{y_d}(t) - \mathbf{C}(\mathbf{x})\mathbf{x}(t)$ and the state and input weighting matrices, $\mathbf{Q}(\mathbf{x})$ and $\mathbf{R}(\mathbf{x})$ respectively, are parameters design that must satisfy requirements: $\mathbf{Q}(\mathbf{x}) \geq 0$ and $\mathbf{R}(\mathbf{x}) > 0\ \forall x$. From equation (15), the Hamiltonian of the suboptimal control problem is given by:

$$\boldsymbol{H}(\boldsymbol{x}, \boldsymbol{u}, \boldsymbol{\lambda}) = \frac{1}{2}[\boldsymbol{y_d}(t) - \boldsymbol{C}(\boldsymbol{x})\boldsymbol{x}(t)]^T\boldsymbol{Q}(\boldsymbol{x})[\boldsymbol{y_d}(t) - \boldsymbol{C}(\boldsymbol{x})\boldsymbol{x}(t)] + \frac{1}{2}\boldsymbol{u}^T(t)\boldsymbol{R}(\boldsymbol{x})\boldsymbol{u}(t) + \boldsymbol{\lambda}^T[\boldsymbol{A}(\boldsymbol{x})\boldsymbol{x}(t) + \boldsymbol{B}(\boldsymbol{x})\boldsymbol{u}(t)],$$

where $\boldsymbol{\lambda}$(t) is a Lagrangian multiplier vector. The minimization of the performance index is guaranteed through optimality conditions:

$$\frac{\partial \mathbf{H}}{\partial \mathbf{u}} = 0; \quad \frac{\partial \mathbf{H}}{\partial \boldsymbol{\lambda}} = \dot{\mathbf{x}}; \quad -\frac{\partial \mathbf{H}}{\partial \mathbf{x}} = \dot{\boldsymbol{\lambda}} \tag{16}$$

and that the matrix $\mathbf{R}(\mathbf{x})$ is positive definite (Naidu (2002)). Expanding the optimality conditions and assuming that there is a linear transformation between the state and the costate ($\boldsymbol{\lambda}$) represented by

$$\boldsymbol{\lambda}(t) = \boldsymbol{P}(\boldsymbol{x})\boldsymbol{x}(t) - \boldsymbol{s}(t),$$

we arrived at the following relations, as demonstrated in (Naidu (2002)):

$$\dot{\boldsymbol{P}}(\boldsymbol{x}) = -\boldsymbol{P}(\boldsymbol{x})\boldsymbol{A}(\boldsymbol{x}) - \boldsymbol{A}^T(\boldsymbol{x})\boldsymbol{P}(\boldsymbol{x}) + \boldsymbol{P}(\boldsymbol{x})\boldsymbol{E}(\boldsymbol{x})\boldsymbol{P}(\boldsymbol{x}) - \boldsymbol{V}(\boldsymbol{x}), \qquad \boldsymbol{P}(\boldsymbol{x}(t_f)) = 0 \tag{17}$$

$$\dot{\boldsymbol{s}}(t) = [\boldsymbol{P}(\boldsymbol{x})\boldsymbol{E}(\boldsymbol{x}) - \boldsymbol{A}^T(\boldsymbol{x})]\boldsymbol{s}(t) - \boldsymbol{W}(\boldsymbol{x})\boldsymbol{y_d}(t), \qquad \boldsymbol{s}(t_f) = 0, \tag{18}$$

where $\boldsymbol{E}(\boldsymbol{x}) = \boldsymbol{B}(\boldsymbol{x})\boldsymbol{R}^{-1}(\boldsymbol{x})\boldsymbol{B}^T(\boldsymbol{x})$, $\boldsymbol{V}(\boldsymbol{x}) = \boldsymbol{C}^T(\boldsymbol{x})\boldsymbol{Q}(\boldsymbol{x})\boldsymbol{C}(\boldsymbol{x})$ and $\boldsymbol{W}(\boldsymbol{x}) = \boldsymbol{C}^T(\boldsymbol{x})\boldsymbol{Q}(\boldsymbol{x})$. It is important to emphasize that the problem refers to the infinite horizon case ($t_f \to \infty$), so the solution of Eq. (17) converges to a constant value of $\boldsymbol{P}$, i.e., it becomes a solution of Riccati's algebraic equation:

$$\mathbf{P}(\mathbf{x})\mathbf{A}(\mathbf{x}) + \mathbf{A}^T(\mathbf{x})\mathbf{P}(\mathbf{x}) - \mathbf{P}(\mathbf{x})\mathbf{E}(\mathbf{x})\mathbf{P}(\mathbf{x}) + \mathbf{V}(\mathbf{x}) = 0 \tag{19}$$

The vector differential equation, Eq. (18), must be solved by backward integration in time, using the boundary condition. An approximation of this solution is shown in paper (Çimen (2007)), also applied in papers (Kuo and Wu (2016)) and (Prach and Tekinalp (2013)), in which

$$\boldsymbol{s}(t) \approx [\boldsymbol{P}(\boldsymbol{x})\boldsymbol{E}(\boldsymbol{x}) - \boldsymbol{A}^T(\boldsymbol{x})]^{-1}(\boldsymbol{W}(\boldsymbol{x})\boldsymbol{y_d}(t)) \tag{20}$$

Thus, the sub-optimal control can be written as

$$\boldsymbol{u}(t) = -\boldsymbol{R}^{-1}(\boldsymbol{x})\boldsymbol{R}^T(\boldsymbol{x})\boldsymbol{\lambda}(t) = -\boldsymbol{K}(\boldsymbol{x})\boldsymbol{x}(t) + \boldsymbol{K_z}(\boldsymbol{x})\boldsymbol{y_d}(t) \tag{21}$$

being: $\boldsymbol{K}(\boldsymbol{x}) = \boldsymbol{R}^{-1}(\boldsymbol{x})\boldsymbol{B}^T(\boldsymbol{x})\boldsymbol{P}(\boldsymbol{x})$ and $\boldsymbol{K_z}(\boldsymbol{x}) = \boldsymbol{R}^{-1}(\boldsymbol{x})\boldsymbol{B}^T[\boldsymbol{P}(\boldsymbol{x})\boldsymbol{E}(\boldsymbol{x}) - \boldsymbol{A}^T(\boldsymbol{x})]^{-1}\boldsymbol{W}(\boldsymbol{x})$.

4. NUMERICAL RESULTS

According to the control strategy and the nonlinear dynamic model defined in the previous sections, the results of the simulations are performed in Matlab® for a quadrotor, whose parameters are shown in the Appendix. The numerical integrator used is the fourth order Runge-Kutta with time step of 0.01s. The control strategy was tested in two trajectories:

- Movement in directions x, y and z simultaneously, with velocity: 0.1 m/s, 0.2 m/s and 0.3 m/s, respectively for 30 seconds and then stay at the position x = 3 m, y = 6 m and z = 9 m.
- Spiral movement with 0.3 m/s of climb speed for 40 seconds. The vehicle must then remain in a circular motion for 10 seconds, without moving in the z direction.

4.1 Rectilinear trajectory

The design parameters of the control system are $k_1 = 7$, $k_2 = 10$, $k_3 = 5$, $\mathbf{Q} = diag(40, 1, 20, 1, 20, 1)$ and $\mathbf{R} = diag(14, 30, 10)$. The results obtained are shown in Fig. 3.

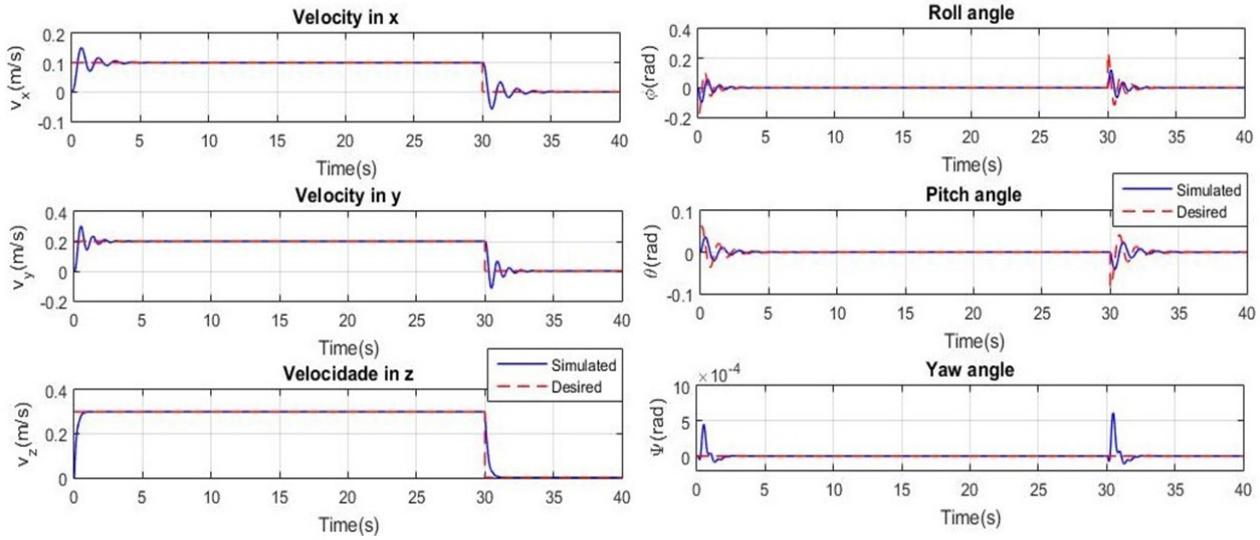

a) Velocities in the x, y and z directions.

b) Behavior of Euler angles.

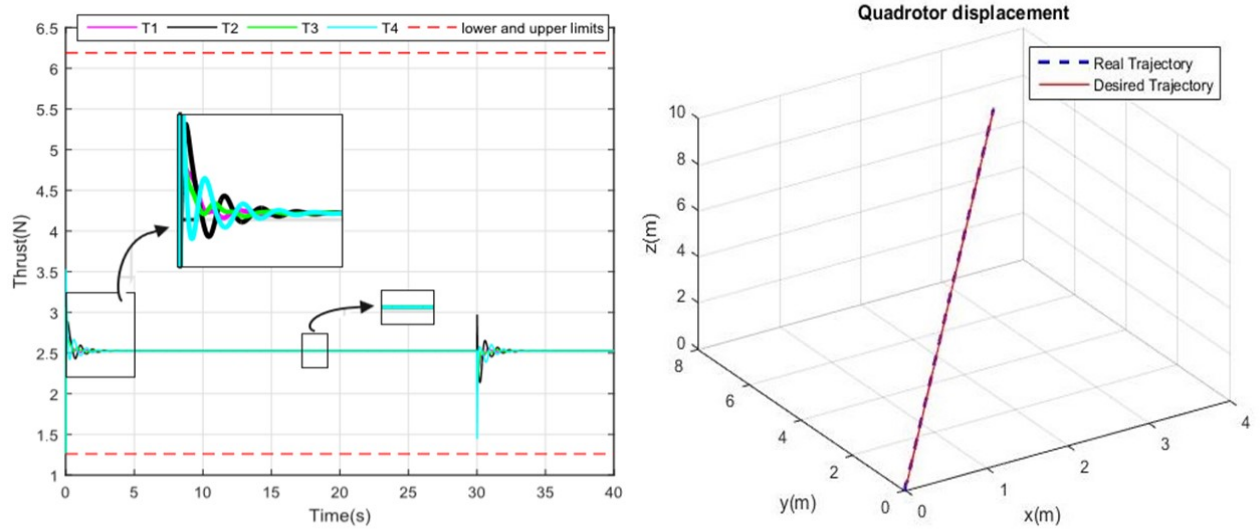

c) Thrust performed by motors.

d) Displacement of the vehicle in three-dimensional space.

Figure 3. Rectilinear trajectory.

The Figure 3 c) shows the behaviour of the thrust performed by the respective motors. After the velocity transitions, U1 (total thrust) is the only control that operates in the system, whose module is exactly equal force weight. Therefore the

thrust values converge to 1/4 of the force weight, i.e., 2.5261 N. The operating range is associated with maximum power and motors shutdown. The first velocities transition generates an error during flight path, which is approximately 1 cm; 2 cm and -2 cm, in x, y and z, respectively. A three-dimensional view of the trajectory is shown in Fig. 3 d), with errors in the final position being 0.3 cm, 0.4 cm, and 2 cm.

4.2 Spiral trajectory

The design parameters of the control system are $k_1 = 7$, $k_2 = 10$, $k_3 = 8$, $\mathbf{Q} = diag(20, 1, 40, 1, 20, 1)$ and $\mathbf{R} = diag(15, 30, 15)$. The result of the simulation obtained is shown in Fig 4. In the XY plane, the circular trajectory executed by the quadrotor is parameterized as a function of time as follows,

$$x = Rcos(\frac{\pi t}{10}), \qquad y = Rsin(\frac{\pi t}{10})$$

so, the reference velocities in the x and y directions are

$$\dot{x}_r = -\frac{R\pi}{10}sin(\frac{\pi t}{10}), \qquad \dot{y}_r = \frac{R\pi}{10}cos(\frac{\pi t}{10}).$$

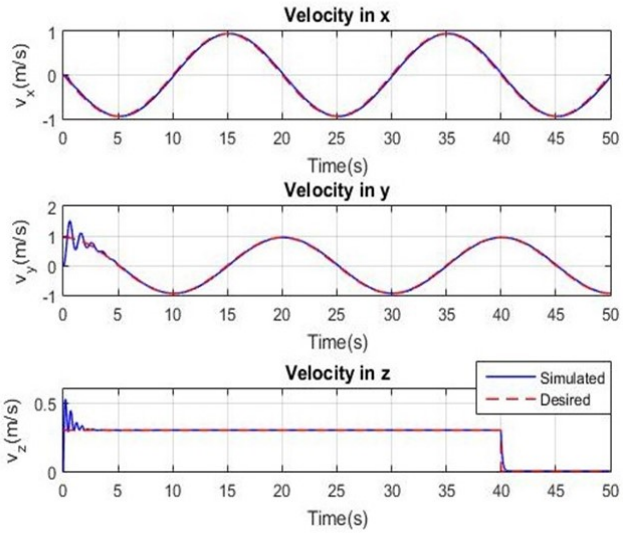

a) Velocities in the x, y and z directions.

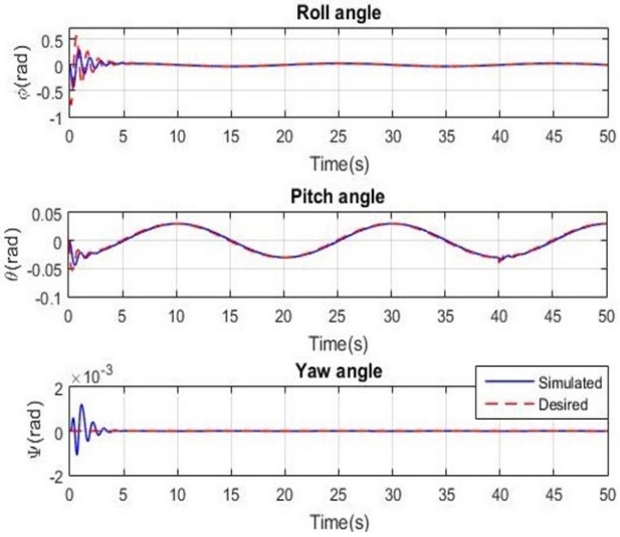

b) Behavior of Euler angles.

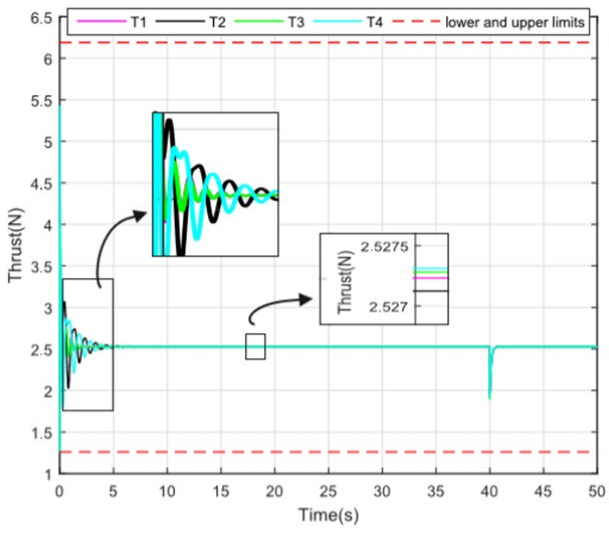

c) Thrust performed by motors.

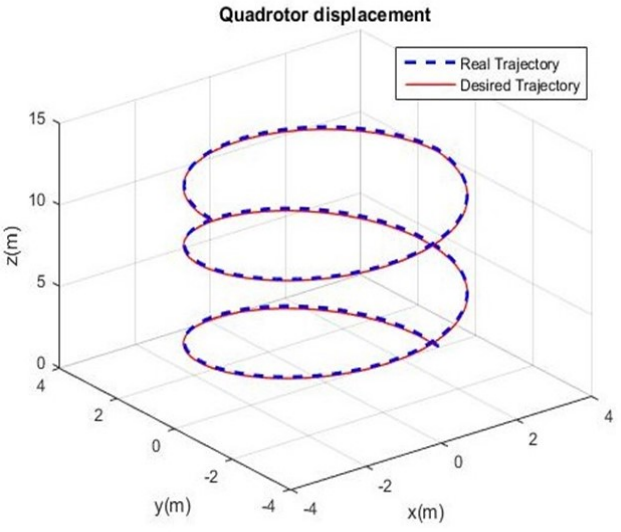

d) Displacement of the vehicle in three-dimensional space.

Figure 4. Spiral trajectory.

Note that the more accented amplitude of the roll angle, as shown in Fig. 4b), results in variations of velocities in the y and z direction during the transient response (approximately 5 seconds), consequently there is an error in the final position in x, y and z of 0.73 cm, 7 cm and 13 cm, respectively. This result can be justified by the coupling of the pitch angle and total thrust with the roll angle, situation derived from the non-simplification of small angular variations. One way to reduce the trajectory error is to increase gains k_1, k_2 and k_3. However, if matrices $\mathbf{Q}$ and $\mathbf{R}$ are kept constant, there is still a wide range of values for the proportional controller gains that can be adjusted to achieve to reduce the error. This gains are related to motor shutdown which occurs for $k_1 = 17$ or $k_3 = 16$, thrust exceeds upper limit for $k_2 = 13$. When one of the motors is turned off, the rotational dynamics of the system becomes uncontrollable.

Different from Fig. 3 c), the Fig. 4 c) shows a small variation of the thrust, of the order 10^{-3}N after 5 seconds, since the vehicle's velocities x and y converge to the reference values, which now depend on time.

In order to determine the influence of the gyroscopic effect, represented by the coefficients c_i (i = 1 to 7) in the rotational dynamic, Eq. (12) to (14), this trajectory is again simulated under the same conditions as before, but now neglecting this effect in the model.

The Fig. 5 shows that there is a small influence of the gyroscopic effect, with the magnitude of the position errors within the order of 10^{-5}m. The reason of this is due to the vehicle's structure that naturally favors the reduction of this effect, i.e., each pair of propellers spins in opposite directions, and each rotor has a small moment of inertia, of the order $10^{-5}kg.m^2$, which justifies this result.

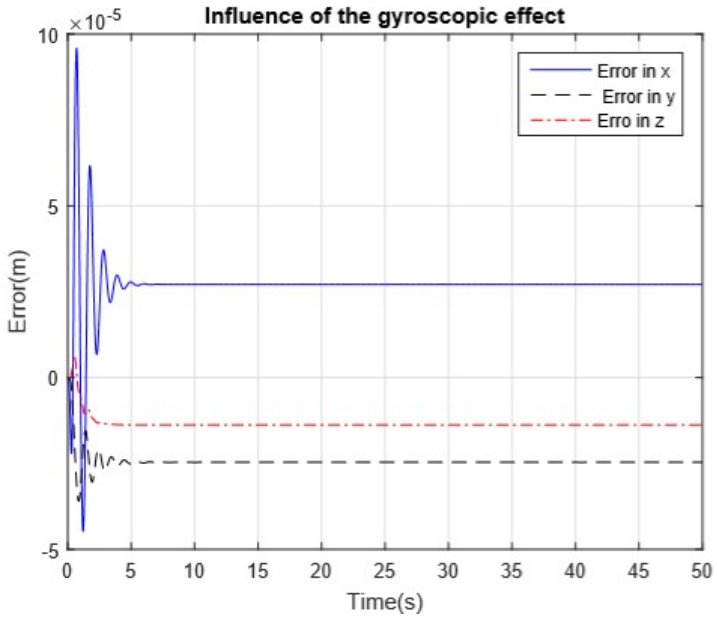

Figure 5. Influence of the term gyroscopic effect.

5. CONCLUSION

In this paper the dynamic model for an Unmanned Aerial Vehicle of the quadrotor type and the design of SDRE and proportional controllers were developed in order to stabilize the attitude of the platform and velocity control, respectively. The analysis was made considering the full nonlinear dynamics, which means, no small-angular variation simplification, thus a strong coupling in the rotational dynamics equations was achieved and dependency on control inputs was preserved. The adopted control strategy was able to control the attitude and velocities of the quadrotor in order to reach the desired flight paths: rectilinear and spiral trajectories. The process of adjusting the proportional controller gains and the weighting matrices was made based on the analysis of simulations until an adequate solution was reached. It was verified a limit for the gains k_1, k_2 and k_3 associated with the thrust operating range. Finally, a small influence of the gyroscopic effect in the spiral trajectory was verified. This result is justified by the fact that the motor has a small moment of inertia (of the order $10^{-5}kg.m^2$), and therefore, it is possible to neglect it in these cases.

6. REFERENCES

Chovancová, A., Fico, T., Chovanec, L. and Hubinský, P., 2014. "Mathematical modelling and parameter identification of quadrotor (a survey)". *Procedia Engineering*, Vol. 96, pp. 172–181.

Çimen, T., 2007. "Approximate nonlinear optimal sdre tracking control." *17th IFAC Symposium on Automatic Control in Aerospace*, Vol. 40, No. 7, pp. 147–152.

Çimen, T., 2008. "State-dependent riccati equation (sdre) control: A survey". In *Proceedings of the 17th World Congress The International Federation of Automatic Control*. Seoul, Korea.

Da Silva, A.L., 2012. "Voo autônomo de veículo aéreo n~ao tripulado tipo quadrirotor". Relatório Final de Pós Doutorado na Universidade de São Paulo.

De Oliveira, A.C.F., 2019. *Modelagem dinâmica e controle de um veículo aéreo não tripulado do tipo quadrirrotor*. Master's thesis, Universidade Federal do ABC, Santo André, Brasil.

Derafa, L., Madani, T. and Benallegue, A., 2006. "Dynamic modelling and experimental identification of four rotors helicopter parameters". In *2006 IEEE International Conference on Industrial Technology*. Mumbai, India.

ElKholy, H.T.M.N., 2014. *Dynamic Modeling and Control of a Quadrotor Using Linear and Nonlinear Approaches*. Master's thesis, The American University in Cairo, Cairo, Egypt.

Kuo, Y.L. and Wu, T.L., 2016. "A suboptimal tracking control approach based on the state-dependent riccati equation method". *Journal of Computational and Theoretical Nanoscience*, Vol. 13, No. 1, pp. 1013–1021.

Lima, G.V., De Souza, R.M.J.A., De Morais, A.S. and De Morais, J.S., 2014. "Modelagem dinâmica de um veículo aéreo não tripulado do tipo quadricóptero". In *XII Conferência de Estudos em Engenharia Elétrica*. Uberlândia, Brazil.

MDIC, 2017. "Estudo sobre a indústria brasileira e europeia de veículos aéreos não tripulados". <http://www.mdic.gov.br/images/publicacao_DRONES-20161130-20012017-web.pdf>.

Mo, H. and Farid, G., 2019. "Nonlinear and adaptive intelligent control techniques for quadrotor uav – a survey". *Asian Journal of Control*, Vol. 21, No. 3, pp. 1–20.

Mracek, C.P. and Cloutier, J.R., 1998. "Control designs for the nonlinear benchmark problem via the state-dependent riccati equation method". *International Journal of Robust and Nonlinear Control*, Vol. 8, pp. 401–433.

Naidu, D.S., 2002. *Optimal Control Systems*. CRC Press, USA, 1st edition.

Nonami, K., Kendoul, F., Suzuki, S., Wang, W. and Nakazawa, D., 2010. *Autonomous Flying Robots: Unmanned Aerial Vehicles and Micro Aerial Vehicles*. Springer, Japan, 1st edition.

Prach, A. and Tekinalp, O., 2013. "Development of a state dependent riccati equation based tracking flight controller for an unmanned aircraft". In *AIAA Guidance, Navigation, and Control (GNC) Conference*. Boston, USA.

Voos, H., 2006. "Nonlinear state-dependent riccati equation control of a quadrotor uav." In *Proceedings of the 2006 IEEE International Conference on Control Applications*. Munich, Germany.

7. APPENDIX

Table 1. Quadrotor's Parameters (Da Silva (2012)).

Parameters	Values	Units
m_t	1.03	kg
L	0.26	m
I_{xx}	$16.83X10^{-3}$	$kg.m^2$
I_{yy}	$16.38X10^{-3}$	$kg.m^2$
I_{zz}	$28.34X10^{-3}$	$kg.m^2$
I_r	$5X10^{-5}$	$kg.m^2$
k_f	$1.4351X10^{-5}$	$N/(rad/s)^2$
k_m	$2.4086X10^{-7}$	$N.m/(rad/s)^2$

8. RESPONSIBILITY NOTICE

The authors are the only responsible for the printed material included in this paper.